A novel magnetizer for 2D broadband characterization of steel sheets and soft magnetic composites

Olivier de La Barrière, Carlo Appino, Fausto Fiorillo, Michel Lécrivain, Carlo Ragusa, Patrice Vallade

A novel magnetizer for 2D broadband characterization of steel sheets and soft magnetic composites

Olivier de la Barrière[1a], Carlo Appino[2], Fausto Fiorillo[2], Michel Lécrivain[1], Carlo Ragusa[3], Patrice Vallade[1]

[1]SATIE, ENS Cachan, CNRS, UniverSud, 61 av du President Wilson, F-94230 Cachan, France
[2]Istituto Nazionale di Ricerca Metrologica (INRIM), Strada delle Cacce 91, 10135 Torino, Italy
[3]Dipartimento Energia, Politecnico di Torino, C.so Duca degli Abruzzi 24, 10129 Torino, Italy

[a] Corresponding author. Electronic address: barriere@satie.ens-cachan.fr, telephone: 0033147402125.

Abstract

The magnetic materials used in embedded applications need characterization and modeling in the kilohertz range. This problem is well addressed under conventional alternating induction, but with rotational and two-dimensional induction loci, which are ubiquitous in electrical machines, there is lack of results, because of the difficult task of reaching such high frequencies at technically interesting induction values with the conventional laboratory test benches. To overcome this difficulty, a novel three phase magnetizer has been designed, exploiting 3D finite element calculations, and applied in the lab. This device permits one to measure magnetization curve and losses in soft magnetic steel sheets and soft magnetic composites under alternating and circular induction up to about 5 kHz. We provide a few significant examples of loss measurements in 0.20 mm thick Fe-Si and $Fe_{50}Co_{50}$ laminations, and in soft magnetic composites. These measurements bring to light the role of skin effect under one- and two-dimensional fields.

I. INTRODUCTION

High speed electrical machines are very promising in terms of torque density [1] and are therefore interesting for embedded applications. But, in order to achieve a correct prediction of the machine efficiency at the design stage, an accurate experimental characterization of the magnetic material in the broad frequency range encountered in such machines, extending up to the kHz range, is needed.

Reaching high frequencies at technically significant induction levels on magnetic characterization benches is far from simple. The necessity of handling large powers with the magnetizing system is a demanding task, especially with two-dimensional (2D) fields. In such a case, no measurement standard is available, in contrast with the conventional characterization under alternating field [2], where one can rely, for example, on ASTM and IEC standards valid up to 10 kHz [3][4]. On the other hand, two-dimensional induction loci are ubiquitous in electrical machines [5] and the 2D magnetic characterization of soft magnetic materials has industrial relevance.

2D measurements are generally performed using either vertical-horizontal double-yoke magnetizers and square samples [6] [7], or a three phase magnetizer with circular/hexagonal samples [8] [9]. While lack of homogeneity of the magnetic induction in the sample can be a problem [10], in all cases the test frequency at technical inductions can barely attain a few hundred Hz, far from actual frequencies encountered in high speed electrical machines.

We discuss in this paper design and operation of a novel 2D broadband three-phase magnetizer, by which superior performances up to the kHz range can be obtained. It is built around a laminated yoke, especially designed through 3D finite element (FEM) calculations. By this device, magnetization curve and losses in magnetic laminations and soft magnetic composite (SMC) materials under alternating and circular induction up to about 5 kHz can be measured. A few significant examples of loss measurements in 0.20 mm thick Fe-Si and $Fe_{50}Co_{50}$ sheets, and in SMC samples are provided and discussed.

II. DESIGN OF THE 2D MAGNETIZER

A) Design constraints

The minimum requirement formulated at start is that the three-phase magnetizer makes possible full

characterization of conventional 0.20 mm thick non-oriented Fe-Si laminations under controlled 2D flux loci up to peak polarization J_p = 1.5 T at the frequency f = 1 kHz. Instrumental to the achievement of this objective is the use of DC-20 kHz CROWN 5000VZ power amplifiers, by which each magnetizing phase can be supplied up to maximum voltage and current peak values $V_{p,MAX}$ = 150 V and $I_{p,MAX}$ = 40 A.

B) Optimizing the magnetizer geometry.

A schematic view of the realized three-phase magnetizer is shown in Fig. 1. For its development, the following design parameters have been imposed: 1) Circular sample of diameter D = 80 mm, expected to exhibit good uniform induction profile, especially in the central region, where the induction and the effective magnetic field are measured [11]. 2) A small airgap, to minimize both the magnetizing current in each phase and the demagnetizing field. An optimal solution, taking into account the mechanical tolerances, is obtained by adopting the airgap width a = 1 mm. 3) Homogeneous rotating field with simplest winding configuration. To this end, the three-phase two-pole stator core was designed with three slots per pole and per phase (totalling 18 slots). To avoid winding overhang crossing, a toroidal winding configuration [11] was adopted (see Fig. 1). 4) Laminated stator core, built out of 0.35 mm thick stacked non-oriented Fe-Si sheets. The details of the windings are given in Fig. 2, where each coil occupies a slot and is series connected with all the other coils of the same phase. If n_S is the number of turns per coil (i.e. the number of conductors per slot), each phase is made of $6 \cdot n_S$ turns in series. To achieve the desired magnetizer performances, the following geometrical parameters, shown in Fig. 1, were optimized: the slot depth t_S, the slot width w_S, the back-core thickness t_Y, and the active axial height T of the core. A convenient number n_S of copper turns per slot was assumed. With maximum magnetizing current density of 5 A/mm^2, as required to avoid overheating, the values t_S = 20 mm and w_S = 5 mm are chosen. At the same time, t_Y is set to 25 mm, making the maximum flux density in the back-core around 0.2 T and the associated energy losses negligible. To calculate the dependence of value and homogeneity of the generated rotating magnetic field and sample induction on the ratio between yoke height and sample thickness T/d, a 3D non-linear magnetostatic FEM modelling is implemented, where the magnetic constitutive equations of yoke sheets and test sample are identified with the corresponding experimental anhysteretic curves. When carrying out such

numerical simulation, the number of turns per slot n_S is not already known, and therefore each coil is modelled by a single copper turn with the magnetomotive force $n_S I_p$. This calculated magnetomotive force per slot $n_S I_p$ providing a defined rotating peak induction B_p = 1.5 T in the 0.20mm thick Fe-Si sample sheet at f = 1 kHz is shown in Fig. 3 as a function of *T/d*. The same figure shows the corresponding trend of the peak flux, normalized to the number of turns per slot φ_p/n_S. which is the sum of the contributions by the six series-connected coils. As expected, the required magnetomotive force $n_S I_p$ decreases with increasing the ratio *T/d*, to reach a more or less asymptotic value beyond $T/d \cong 80$. Here the effect of flux fringing becomes negligible and the quantity φ_p/n_S tends to rapidly increase with *T/d*, following the corresponding increase of the cross-sectional area of the core. Given these trends of $n_S I_p$ and φ_p/n_S, their product $\varphi_p I_p$, that is the apparent power $\pi f \varphi_p I_p$, passes through a minimum. This occurs for $T/d \cong 75$ (corresponding to T = 15 mm), where the normalized flux $\varphi_p/n_S \cong$ 2 mWb and $n_S I_p \cong 100$ A. Consequently, one obtains that the normalized peak voltage at 1 kHz is $V_p/n_S = 2\pi f \varphi_p/n_S \cong 12.6$ V. With I_p = 10 A and n_S = 10, the voltage drop V_p = 127 V is safely within the power supply capabilities. Higher frequencies can actually be reached by changing n_S = 10 to n_S = 5 via a mid-point connection predisposed on each coil. The accordingly built three-phase magnetizer, which is endowed with an air-cooling system, is shown in Fig. 4. It has been tested using a calibrated hysteresisgraph-wattmeter, where a defined 2D induction loci can be imposed by digital feedback [13]. Fig. 5 compares recorded and FEM calculated current and voltage waveforms in one phase of the magnetizer at f = 1 kHz under imposed circular induction of amplitude B_p = 1.0 T. This is detected upon a 20 mm wide central region of the 80mm diameter 0.20 mm thick Fe-Si sample. It is observed that the current waveform is accurately predicted by the FEM calculations, whereas the voltage drop is slightly underestimated. This is due to the fact that the actual windings have somewhat higher overhang than the idealized windings considered in the FEM analysis (see Fig. 1), because of the mechanical rigidity of the copper wire. This implies higher inductance, that is higher voltage drop, than predicted by the numerical model, but no practical consequences on the stated objectives of the design are observed.

III. RESULTS: A FEW EXAMPLES

Test measurements have been performed on Fe-Si and Fe-Co sheets and on soft magnetic composites with

the fieldmetric method [8]. For measurements beyond a few hundred Hz, the employed *H*-coil is wound with well separated turns, minimizing the stray capacitances. The 3D FEM analysis shows that upon the central 20 mm measuring square region of the disk samples the homogeneity of the effective field is better than 2 %.

The non-oriented Fe-Si and Fe-Co 0.20 mm thick sheets have been characterized under alternating and rotating field up to J_p = 1.55 T at f = 2 kHz and J_p = 2.1 T at f = 5 kHz, respectively. An example of measured alternating $W^{(ALT)}$ and rotational $W^{(ROT)}$ energy loss behaviour versus frequency and peak polarization J_p in the Fe-Co sheets is shown in Fig. 6a. It is noted how the maximum of the rotational loss occurs at increasing J_p values with increasing the magnetizing frequency. This occurs because of the increasing proportion of the classical loss component W_{class}, which, contrary to the other components, the domain wall related hysteresis W_{hyst} and excess W_{exc} losses, monotonically increases with J_p [8]. However, loss separation is not easily treated under broadband conditions, because skin effect may arise and the standard equation of the classical energy loss, which is written as $W_{class}(J_p, f) = k\frac{\pi^2}{6}\cdot\sigma d^2 B_p^2 f$, where σ is the conductivity (k = 1 for alternating sinusoidal induction , k = 2 for circular induction) will not apply beyond a certain upper frequency f_{lim}. It is indeed interesting to see how one can easily find f_{lim} by loss separation. It is a unique simple way to detect the surge of the skin effect. According to the statistical theory of losses and the previous equation for W_{class}, it is predicted that $W_{diff} = W_{hyst} + W_{exc}$ is proportional to $f^{1/2}$ [13]. Fig. 6b, showing the behaviour of W_{diff} at J_p = 1 T versus $f^{1/2}$ up to f = 5 kHz, shows that such a prediction is satisfied up to $f = f_{lim} \cong 400$ Hz. Beyond this frequency, W_{class} is overestimated by the previous equation and the calculated W_{diff} strongly deviates from the $f^{1/2}$ behavior. At higher induction levels, this tendency can be reversed as shown in [15] [16], W_{class} being underestimated by the previous formula. As explained in [15], this is an effect of saturation, which deeply changes the induction repartition over the sample cross section at high induction levels.

Further experiments have been performed on SMC samples. These materials are made of bonded and pressed iron particles, typically 10 μm to 100 μm wide. Because of their isotropic properties, they can handle 3D fluxes, besides being attractive for high frequency applications. Fig. 7 shows an example of energy loss versus frequency measured under alternating (sinusoidal) and circular polarization up to 4 kHz, in 80 mm diameter 3

mm thick disk samples (see [17] [18] for more details). The non-linear increase of $W^{(ALT)}$ and $W^{(ROT)}$ with f can be observed also in these materials. The relatively large sample thickness, required for mechanical reasons, combines with intrinsically low permeability values to impose, for a same apparent power of the magnetizing system, pretty lower $J_p \cdot f_{max}$ products than in sheet samples. Examples of such limits are $J_p \cdot f_{max}$ = 1.25 T·1 kHz or $J_p \cdot f_{max}$ = 1.0 T·2 kHz. They are nonetheless quite larger than those obtained in the recent literature (e.g. $J_p \cdot f_{max}$ = 0.77 T·1 kHz) [19].

IV. CONCLUSIONS

A new magnetizer, associated with digitally controlled hysteresisgraph/wattmeter, has been developed for the broadband alternating and two-dimensional characterization of soft magnetic sheets and composites deep into the kHz range. This device, largely overcoming the upper polarization and frequency limits reported so far in the literature for similar apparatus, has been designed and optimized by 3D FEM calculations. With the high frequency range made available to the 2D measurements, the skin effect in magnetic laminations under rotating induction has been unambiguously put in evidence for the first time. The non-linear increase of the energy loss with the magnetizing frequency is also demonstrated in the soft magnetic composites.

References

[1] S. Niu, . Ho, W. Fu, and J. Zhu, Eddy current reduction in High-Speed Machines and Eddy Current Loss Analysis With Multislice Time-Stepping Finite-Element Method, *IEEE Trans. Magn.*, **48** (2012), 1007-1010.

[2] C. Appino, E. Ferrara, F. Fiorillo, L. Rocchino, C. Ragusa, J. Sievert, T. Belgrand, C. Wang, P. Denke, S. Siebert, Y. Norgren, K. Gramm, S. Norman, R. Lyke, M. Albrecht, X. Zhou, W. Fan, X. Guo, M. Hall, International comparison on SST and Epstein measurements in grain-oriented Fe-Si sheet steel, *International Journal of Applied Electromagnetics and Mechanics*, in press.

[3] IEC Standard Publication 60404-10, Methods of measurement of magnetic properties of magnetic steel sheet and strip at medium frequencies, 1988, Geneva, IEC Central Office.

[4] ASTM Publication A348/A348M, Standard test method for alternating current magnetic properties of materials using the wattmeter-ammeter-voltmeter method, 100 to 10 000 Hz and 25-cm Epstein frame, 2011, West Conshohocken, PA.

[5] O. Bottauscio, M. Chiampi, A. Manzin, M. Zucca, Additional losses in induction machines under synchronous no-load conditions, *IEEE Trans. Magn.*, **40** (2004) 3254-3261.

[6] J.G. Zhu and V.S. Ramsden, *IEEE Trans. Magn.*, **29** (1993) 2995-2997.

[7] A.J. Moses, Rotational magnetization-problems in experimental and theoretical studies of electrical steels and amorphous magnetic materials, *IEEE Trans. Magn.*, **30** (1994) 902-906.

[8] C. Appino, F. Fiorillo, and C. Ragusa, One-dimensional/two-dimensional loss measurements up to high inductions, *J. Appl. Phys.* **105** (2009), 07E718.

[9] A. Hasenzagl, B. Weiser, and H. Pfützner, Novel 3-phase excited single sheet tester for rotational magnetization, *J. Magn. Magn. Mater.*, **160** (1996) 180-182.

[10] N. Nencib, A. Kedous-Lebouc, B. Cornut, 2D analysis of rotational loss tester, *IEEE Trans. Magn.*, **31** (1995) 3388-3390.

[11] Y. Guo, J. Zhu, J. Zhong, H. Lu, and J. Jin, Measurement and modeling of rotational core losses of soft magnetic materials used in electrical machines: a review, *IEEE Trans. Magn.*, **44** (2008), 279-291.

[12] R. Qu, M. Aydin, and T.A. Lipo, Performance comparison of dual-rotor radial-flux and axial-flux permanent-magnet BLDC machines, *in IEEE Electric Machines and Drives Conference (IEMDC)*, 2003.

[13] C. Ragusa and F. Fiorillo, A three-phase single sheet tester with digital control of flux loci based on the contraction mapping principle, *J. Magn. Magn. Mater.*, vol. 304, no. 2 (2006), pp. e568-e570.

[14] G. Bertotti, General properties of power losses in soft ferromagnetic materials, *IEEE Trans. Magn.*, **24** (1988) 621-630.

[15] C. Appino, O. de la Barrière, C. Beatrice, F. Fiorillo, C. Ragusa, Rotational magnetic losses in nonoriented Fe–Si and Fe–Co laminations up to the kilohertz range, *IEEE Trans. Magn.*, **50** (2014), 2007104.

[16] C. Appino, O. Hamrit, F. Fiorillo, C. Ragusa, O. de la Barrière, F. Mazaleyrat, M. LoBue, Skin effect in steel sheets under rotating induction, *International Journal of Applied Electromagnetics and Mechanics*, in press.

[17] O. de la Barrière, C. Appino, F. Fiorillo, C. Ragusa, M. Lecrivain, L. Rocchino, H. Ben Ahmed, M. Gabsi, F. Mazaleyrat, M. LoBue, Extended frequency analysis of magnetic losses under rotating induction in soft magnetic composites, *J. Appl. Phys.*, **111** (2012), 07E325.

[18] O. de la Barrière, C. Appino, C. Ragusa, F. Fiorillo, F. Mazaleyrat, M. LoBue, High-frequency rotational losses in different soft magnetic composites, *J. Appl. Phys.*, **115** (2014), 17A331.

[19] Y. Guo, J. Zhu, H. Lu, Z. Lin, and Y. Li, Core Loss Calculation for Soft Magnetic Composite Electrical Machines, *IEEE Trans. Magn.*, **48** (2012) 3112-3115.

Figures captions

Fig. 1. 3D finite element model of the three-phase magnetizer and its main geometrical parameters.

Fig. 2. Details of the three phase magnetizer windings.

Fig. 3. Magnetomotive force per slot $n_S I_p$ and resulting peak flux per turn φ_p/n_S as a function of core to sample thickness ratio T/d for a rotating peak induction B_p = 1.5 T at f = 1 kHz in a 0.20 mm thick non-oriented Fe-Si sheet sample. Minimum supply power $\pi f \varphi_p I_p$ is required for $T/d \cong 75$.

Fig. 4. The realized 2D three-phase magnetizer.

Fig. 5. Measured and FEM calculated current $i(t)$ circulating in a phase of the stator and corresponding voltage $v(t)$ waveforms for rotating induction B_p = 1 T at 1 kHz in a 0.20 mm thick non-oriented Fe-Si sheet sample.

Fig. 6. Examples of alternating ($W^{(ALT)}$) and rotational ($W^{(ROT)}$) energy loss measurements performed with the novel 2D broadband magnetizer. (a) $W^{(ALT)}$ and $W^{(ROT)}$ measured at three different frequencies in a 0.20 mm thick Fe-Co sheet sample versus peak polarization. (b) The quantity $W_{diff} = W - W_{class}$, where W_{class} is the classical loss calculated according to the standard formula for uniform induction in the sample cross-section, shows strong deviation from the expected linear dependence on $f^{1/2}$ beyond about 400 Hz, signaling the surge of the skin-effect.

Fig. 7. Alternating and rotational energy loss versus frequency at different polarization values in a commercial soft magnetic composite. The measurements are performed on 80 mm diameter 3 mm thick disk samples.

Figures

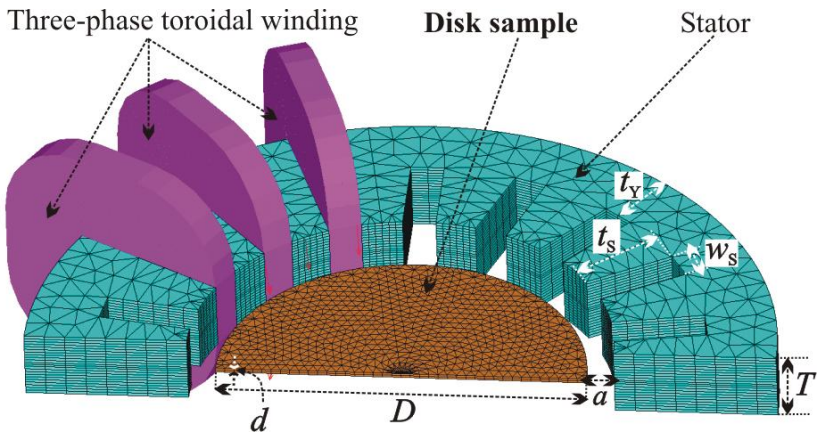

Fig. 1

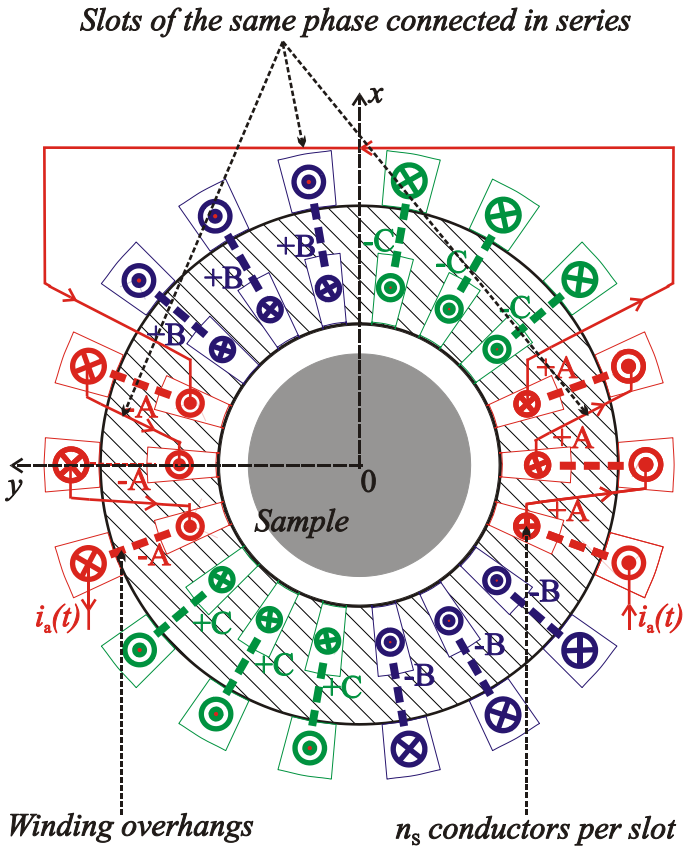
Slots of the same phase connected in series
x
y
0
Sample
+B
-C
+A
-A
+C
-B
$i_a(t)$
Winding overhangs
n_s conductors per slot

205
206

Fig. 2

207

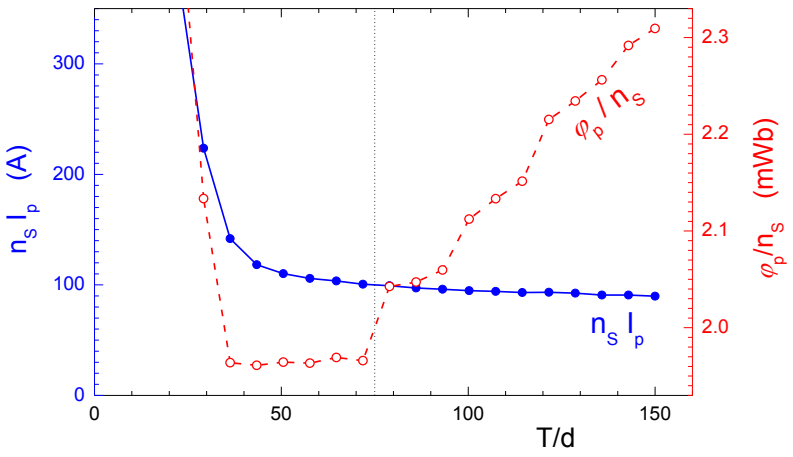

208

209 Fig. 3

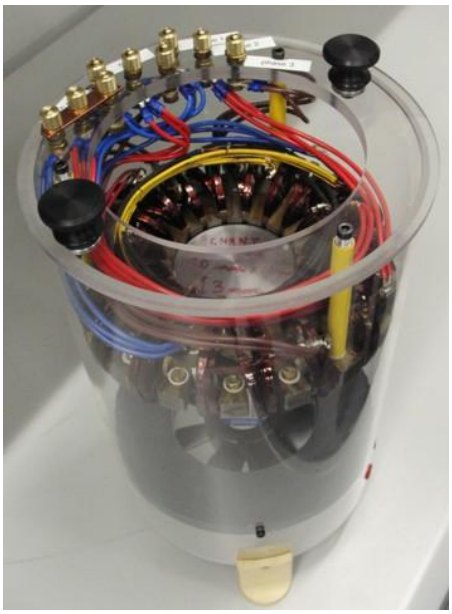

Fig. 4

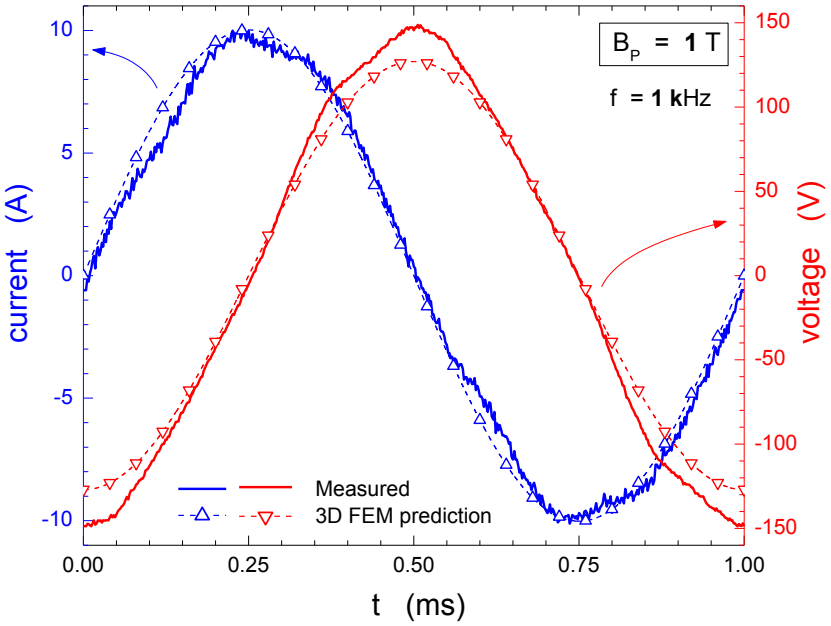
B_P = 1 T
f = 1 kHz
current (A)
voltage (V)
t (ms)
Measured
3D FEM prediction
10
5
0
-5
-10
150
100
50
0
-50
-100
-150
0.00
0.25
0.50
0.75
1.00

212

213 Fig. 5

214

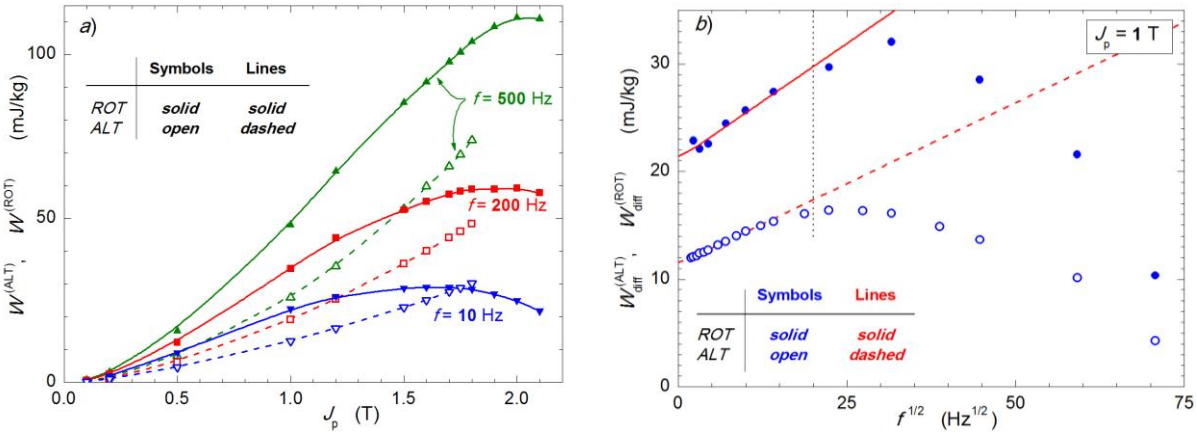
a)
Symbols
Lines
ROT
ALT
solid
open
solid
dashed
f = 500 Hz
f = 200 Hz
f = 10 Hz
W(ALT), W(ROT) (mJ/kg)
Jp (T)
b)
Jp = 1 T
Wdiff(ALT), Wdiff(ROT) (mJ/kg)
f 1/2 (Hz1/2)

215 Fig. 6

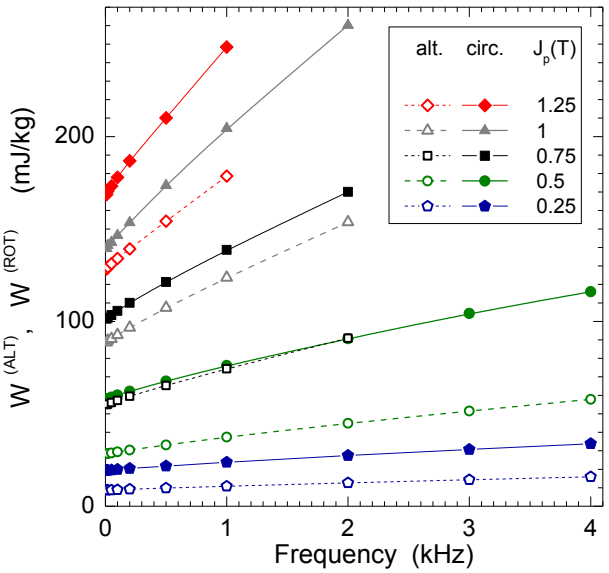
alt. circ. J_p(T)
1.25
1
0.75
0.5
0.25
$W^{(ALT)}$, $W^{(ROT)}$ (mJ/kg)
200
100
0
0
1
2
3
4
Frequency (kHz)

Fig. 7